LBL-35903

Lawrence Berkeley Laboratory
UNIVERSITY OF CALIFORNIA

Physics Division

To be presented at the Seventh Annual Conference on Biomedical Engineering, Tehran, Iran, December 18–21, 1994, and to be published in the Proceedings

Medical Imaging Applications of Amorphous Silicon

A. Mireshghi, J. Drewery, W.S. Hong, T. Jing, S.N. Kaplan, H.K. Lee, and V. Perez-Mendez

July 1994

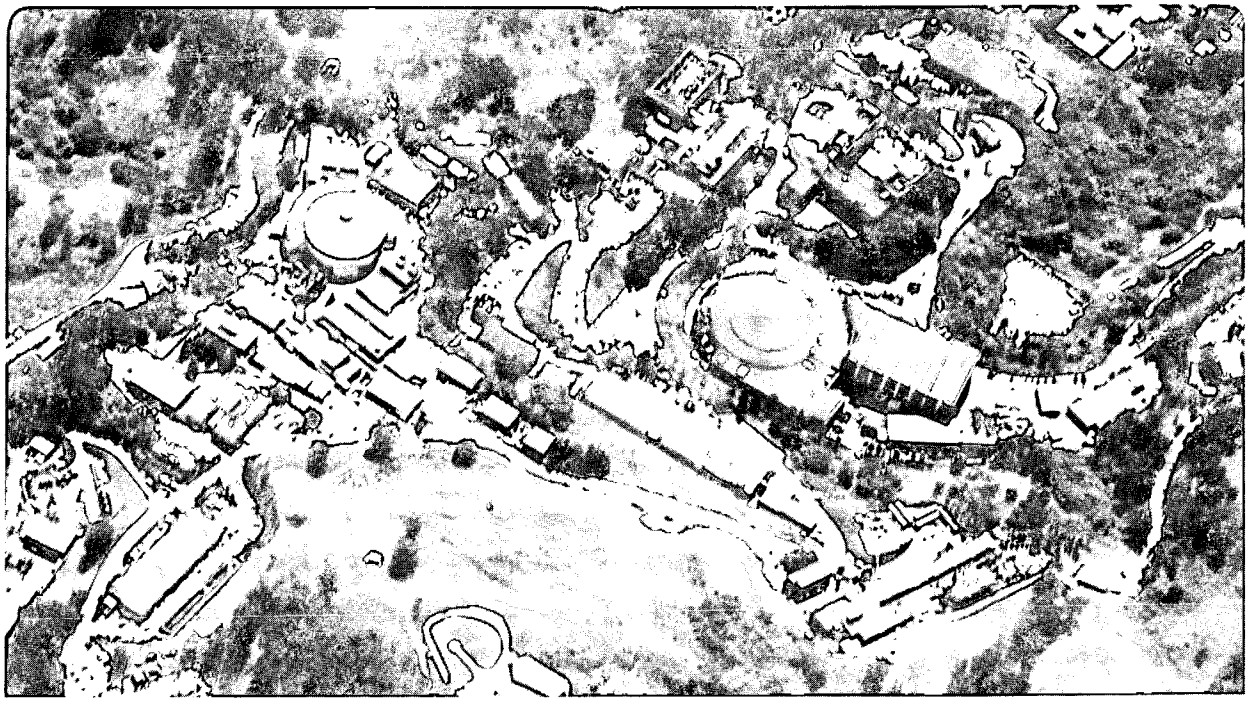

Prepared for the U.S. Department of Energy under Contract Number DE-AC03-76SF00098

DISCLAIMER

To be presented at 7th Annual Conference on Biomedical Engineering, December 1994, Tehran, Iran

LBL-35903

MEDICAL IMAGING APPLICATIONS OF AMORPHOUS SILICON

A. Mireshghi, J. Drewery, W.S. Hong, T. Jing, S.N. Kaplan, H.K. Lee
and V. Perez-Mendez

Physics Division
Lawrence Berkeley Laboratory*
University of California
Berkeley, CA 94720

JULY 1994

---

*This work was supported by the Director, Office of Energy Research, Office of High energy Nuclear Physics, High Energy Physics Division of U.S. Department of Energy under Contract Number DE-AC03-76SF00098

MEDICAL IMAGING APPLICATIONS OF AMORPHOUS SILICON

A. Mireshghi*, J. S. Drewery, W. S. Hong, T. Jing, S.N. Kaplan, H. K. Lee and V. Perez -Mendez

Lawrence Berkeley Laboratory, University of California, Berkeley , CA 94720

Abstract

Two dimensional hydrogenated amorphous silicon (a-Si:H) pixel arrays are good candidates as flat-panel imagers for applications in medical imaging. Various performance characteristics of these imagers are reviewed and compared with currently used equipments. An important component in the a-Si:H imager is the scintillator screen. A new approach for fabrication of high resolution CsI(Tl) scintillator layers, appropriate for coupling to a-Si:H arrays, are presented. For nuclear medicine applications, a new a-Si:H based gamma camera is introduced and Monte Carlo simulation is used to evaluate its performance.

I. INTRODUCTION

Hydrogenated amorphous silicon (a-Si:H) films can be coated on a variety of substrate materials using various deposition techniques. It is commonly produced by decomposition of silane gas in plasma enhanced chemical vapor deposition (PE-CVD) machines. The usefulness of this material in electronic applications was recognized in 1976, when the possibility of doping of this material, and therefore, making p-n junctions was reported.[1] Since then it has been the most widely used material for solar cells and has also been used as thin film transistor (TFT) switches in fax machine heads, flat monitor screens, and electrocopying machines.[2] Radiation detection applications of a-Si:H for X and γ rays, neutrons, and charged particles are established.[3,4,5] As a detector for nuclear radiation or light,(solar cell) a-Si:H material is used in the form of reverse biased n-i-p diodes. The intrinsic layer is the radiation sensitive part and in photodiodes; it needs to be made 0.5-1 μm thick. The n and p layers are produced by addition of small concentrations of phosphine (PH_3) and diborane (B_2H_6) to the main process gas (silane), and are normally made about 20-30 nm thick. The choice of substrate depends on the application, For radiation detectors Corning 7059 glass or Kapton can be used. Metallic contacts are usually vacuum-coated or sputtered thin chromium layers or, light transparent indium tin oxide (ITO) films. For X and γ rays detection, a layer of a proper phosphor material is required to convert the incident radiation to visible light, which produces electron hole pairs in the intrinsic layer of the a-Si:H photodiode. Recently development of large area X and γ ray imagers and their associated electronic readouts have been reported.[6,7] Although certain electronic characteristics of a-Si:H are inferior to crystal silicon, the possibility of making low cost large area devices, as well as its inherent radiation hardness, makes it advantageous in many imaging applications. Recently we have shown that certain electronic properties of a-Si:H are improved by hydrogen dilution of the process gas.[8]

In this paper we review applications of a-Si:H photodiodes in medical radiography and nuclear medicine, present our scheme for enhancing spatial resolution of CsI(Tl) scintillator layers, and also discuss simulation results on the performance of our prototype a-Si:H based gamma camera.

II. MEDICAL IMAGING

Various forms of digital radiography have been utilized for certain medical applications over the last two decades, using the conventional radiographic films or image intensifier tubes. During the last few years the development of large area and high density a-Si:H pixel arrays has provided a potential for real time imaging that may soon be able to completely supplant X-ray screen film. Although the newly developed 1536x1920 pixels a-Si:H sensor arrays with a pixel pitch of 127 μm [7] does not yet offer the spatial resolution comparable to radiographic films, it proves to be superior to the current real time imaging technologies in many aspects. The existing system used in fluoroscopy utilizes image intensifier tubes with CsI(Na) X-ray sensitive layers, to form an image on a small solid state detector, such as a charged coupled device (CCD). Image intensifier tubes are very reliable, but they have the some disadvantages due their bulk, high cost, and low resolution, resulting from imperfect electron optics and loss of sharpness in optical couplings. In the real time imaging of megavoltage photon treatment beams (^{60}Co, or 3 to 50 MV X-ray) used in cancer therapy, demand for resolution is modest, ~1 lp/mm. and therefore a pixel pitch of ~ 500 μm is sufficient. For diagnostic X-ray imaging (~25 to 150 KVp), a resolution of 4-5 lp/mm is required to compete with most routine radiographic and fluoroscopic equipments. A-Si:H based two dimensional arrays with pixel pitch of 127 μm reported in ref. nearly provides this resolution. Considering the exponential increase in the pixel counts per imaging array trend with time [6], the outlook for the future of this technology is even brighter. Other performance characteristics of a-Si:H based imagers are: signal to noise ratio, linearity, readout speed, and image lag. The latter two are important in X-ray fluoroscopy and are addressed in ref. 9. It has been shown that the high resolution a-Si:H arrays are capable of providing fluoroscopic images at rates of at least 30 frames per second. For diagnostic medical X-ray, assuming an exposure of 0.1 R, approximately 10^{12} visible photons/cm^2 are created in the scintillator, which results in a large signal charge of ~ 10^4 fC for a 100x100 μm^2 pixel, therefore

*On leave from Sharif University of Technology, Tehran, Iran

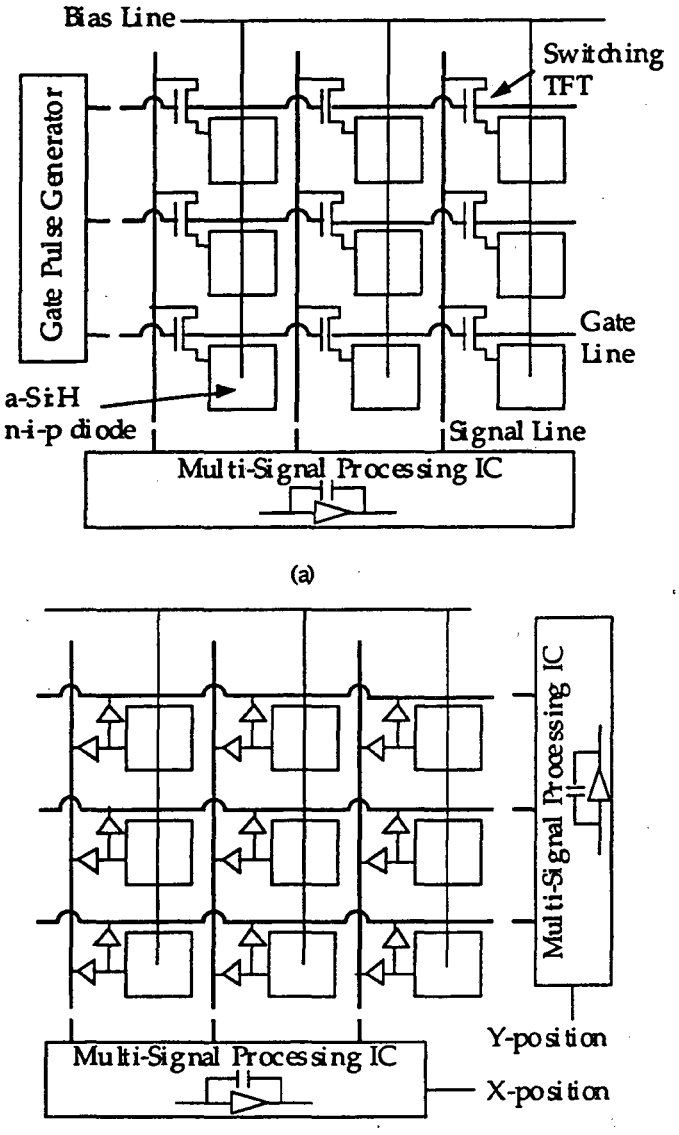

Fig. 1 Schematic diagram of a-Si:H pixel array with readout electronics. (a) Image scanning readout, (b) position detecting readout for event-by-event collection mode.

providing an excellent dynamic range for this kind of application. The response linearity of a-Si:H imaging pixels at a reverse bias ~ 2.5 volts is better than 1% for more than 85% of the full signal range.[10] The application of the a-Si:H arrays for tomographic imaging has also been investigated and their adequacy for acquiring X-ray transmission scan for attenuation correction in PET and SPECT imaging is reported. [11]

The new generation of X-ray imagers consist of two major components, (a) phosphor screens, and (b) photosensitive detector arrays. In a phosphor material, electron-hole pairs produced by interaction of incoming radiation recombine to generate visible photons. For X-ray conversion, several scintillator screens such as, Lanex (Kodak) and Chronex (Dupont) are commercially available. Better light collimations can be obtained by fiber optic plates with rare earth scintillators such as, terbium or cerium, with fiber sizes as small as 20 μm.[12] A more appropriate scintillator for coupling to a-Si:H photo-diodes is CsI(Tl). Below, we will discuss Vacuum evaporated CsI(Tl) scintillator layers with columnar structure developed here at LBL.

Semiconductor photo sensitive arrays such as, CCD and silicon p-n junction photo-diodes arrays (PDA) are widely used today. A major disadvantage of these devices is the small array size of 3x5 cm^2 which restricts their applications for most medical radiation imaging.[13] A-Si:H sensor arrays are now considered as advantageous alternatives for medical imaging applications. In the following, some insight into the structure and operation of these arrays will be given .

A. A-Si:H Pixel Arrays

Amorphous silicon photodiodes can be integrated with their readout electronics on large area substrates to form pixel arrays with two dimensional position sensitivity. In these arrays, in order to achieve a high fill factor,(radiation sensitive fraction of the total pixel area) each pixel photodiode is deposited on the top of its associated TFT switch or amplifier. With today's technology, 30x30 cm^2 arrays with pixel sizes of 100x100 μm^2 are achievable, and arrays as large as 60x60 cm^2 are predicted to be available by the end of the decade.[6]

Depending on the mode of operation, two different schemes for signal readout are applicable, (a) image scanning, and (b) position detection readout.[14] In the scanning mode, (Fig. 1a) signal charge is stored on the pixel capacitance during the off period of the TFT switch. The stored charge is later read out by turning the TFT on, so that the signal charge can be transferred, through a data line, to a charge sensitive amplifier. All pixels in a row have a common gate line, and all pixels in a column share a single data line. Scanning is performed by sending sequential pulses to the gate lines, and after each pulse, reading output from the amplifiers connected to the data lines successively. In the position detection readout (Fig. 1b) scheme, each pixel has its own charge sensitive amplifier which sends output to both an X and Y data line. Each incoming photon on the array may produce signal charges in several adjacent pixels. The X and Y lines producing the largest signal identify the position of the incident photon.

B. Enhanced Resolution CsI(Tl) Phosphor

CsI(Tl) is known to be the most efficient scintillator for charged particles and for X-radiation and can emit more than 60,000 photons /MeV absorbed energy, under optimal conditions.[15] As shown in Fig.2, the peak emission of this scintillator is about 580 nm, which coincides very well with the peak collection efficiency of a-Si:H. However, for a photo-diode array coupled to a CsI(Tl) converter layer, the spatial resolution will be restricted by the diffusion of photo luminescent photons within the scintillator layer, if proper collimation of light does not occur. We have developed a new approach for the fabrication of CsI(Tl) layers which results in

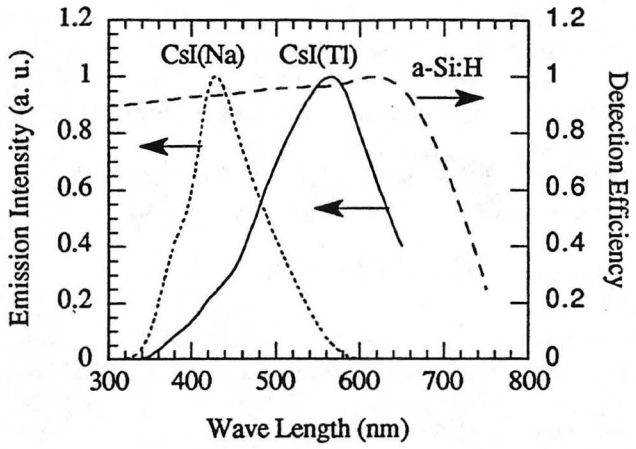

Fig.2 Emission spectra of CsI(Tl), CsI(Na), and a-Si:H response

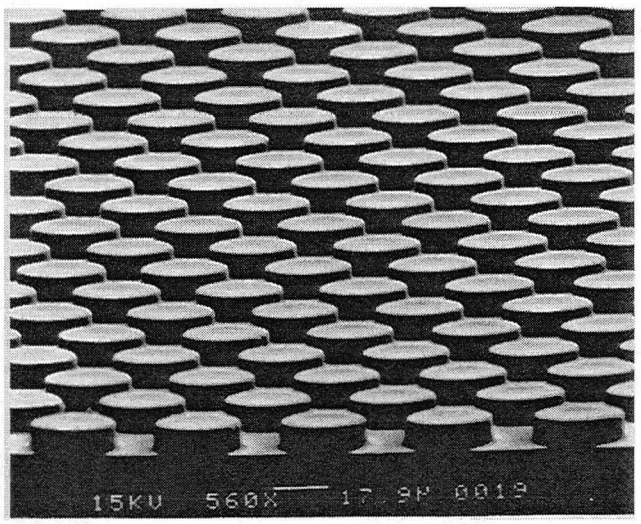

Fig. 3 SEM of a patterned substrate used for CsI(Tl) coating.

formation of a sequence of columns of regular, controlled size (diameter) perpendicular to the substrate (detector).[16,17] This structure provides the scintillator with a light collimation which improves radiation detection resolution. Formation of the columns are enhanced by evaporating the scintillator on a patterned substrate. The substrate shown in Fig. 3 is a thin (10-15 μm) polyimide coated on Si wafer and then patterned using standard photo lithographic techniques. The CsI (Tl) layer is then vacuum evaporated using CsI and $TlCl_2$ powders in two separate boats and operated at different temperatures, in order to control the Tl to CsI composition ratio.[17] For an optimum light yield, a minimum Tl activator molecular concentration of 0.2 % is required. Figure 4 shows SEM (scanning electron microscope) micrographs of CsI(Tl) layers deposited on patterned substrates, (a) before and (b) after annealing at 500 ^{o}C. As seen, the annealing reduces the spreading of columns near the top and also widens the gap between columns, hence, further enhancing the light collimation of the structure. In Fig.5 we show the modulation transfer function (MTF) for (a) Lanex fast screen, (b) non-

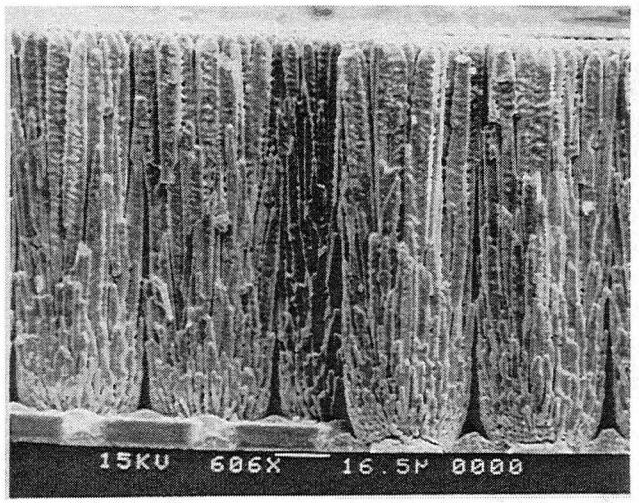

(a)

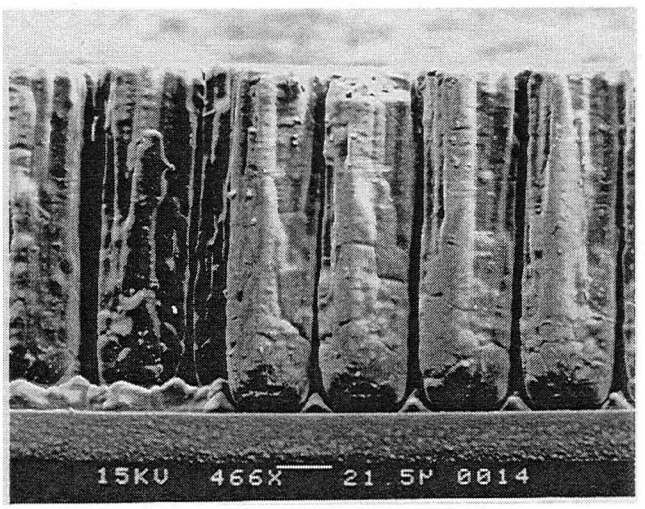

(b)

Fig.4 SEM of CsI(Tl) layers deposited on patterned substrates, (a) columnar structure before annealing, (b) after annealing at 500 ^{o}C.

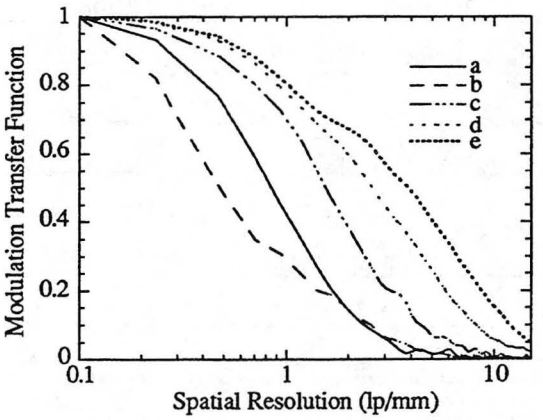

Fig. 5 Modulation Transfer functions for (a) Lanex fast screen, (b) non-structured CsI(Tl) crystal 200 μm thick, (c) structured CsI(Tl) layer 220 μm thick, (d) Lanex fine screen 75 μm thick, (e) structured CsI(Tl) layer 75 μm thick.

structured CsI(Tl) crystal 220 μm thick, (c) structured CsI(Tl) layer 220 μm thick, (d) Lanex fine screen 75 μm thick, and (e) structured CsI(Tl) layer 75 μm thick.[17] As seen, the structured CsI(Tl) layers (c and e) show a substantial improvement over those of the Lanex screens and non-structured CsI(Tl) layer. The spatial resolution at 10% level for curve (e) is ~ 12 lp/mm. As a comparison, a structured CsI(Tl) layer ~ 110 μm thick produces more than twice as much light as a Kodak Lanex fine screen with an equivalent resolution does. The evaporated CsI(Tl) layer is more resistant to radiation damage than a crystal; its light output is only reduced by a factor of 2 after exposure to 10^4 Gy of exposure to Co-60 γ rays. More detailed measurement and analysis of the structured CsI(Tl) scintillator layers may be found in refs. 16,17. The result of these studies indicate that such a scintillator layer is a good candidate for coupling to an a-Si:H pixel array to be used in medical imaging.

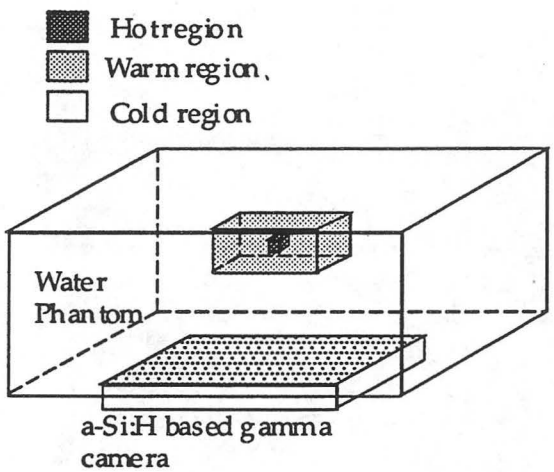

Fig. 6 The geometry of the water phantom with hot, warm and cold sources

Table I. Parameters of the water phantom and the detector.

Cold region	size = 30 x 30 x 15 cm^3, 0 kBq/ml
Warm region	size = 8 x 4 x 4 cm^3, 83.5 kBq/ml
Hot region	size = 8 x 8 x 8 mm^3, 918.5 kBq/ml
γ source	^{99m}Tc or ^{201}Tl
Distance	7 cm between phantom and collimator
Scintillator	2 mm or 5 mm thick CsI(Tl)
detector area	12.8 x 12.8 cm^2
No. of pixels	128 x 128 with pixel size of 1 x 1mm^2

III. NUCLEAR MEDICINE

The conventional device currently used in nuclear medicine is an improved version of the so-called "Anger Camera",[18] which consists of a collimator, NaI scintillator, photo-multiplier tubes (PMT), and position sensing circuitry. The resolution is limited by the thickness requirement of the scintillator and is normally not better than 3 mm FWHM. A gamma camera based on a-Si:H pixel arrays and CsI(Tl) scintillator would have several advantages such as, higher resolution, compactness, portability and lower cost.

A. A-Si:H based Gamma Camera

In nuclear medicine, the requirements of the imaging devices are different from diagnostic and MV X-ray treatment imaging. In this application, the most widely used source is ^{99m}Tc, and during the 3 minute data acquisition by the camera, not more than ~ 10^6 γ rays is acquired from 20x20 mm^2 area of the body. This results in a γ ray fluence of ~2500 140 keV photons/cm^2, and will produce about 10^7 visible photons/cm2 in scintillator and a similar number of electron-hole pairs in the photodiode. Therefore, a 3 minute stored signal charge of ~ 10 fC per mm^2 for the sensitive area of a pixel is expected, which is well above the noise. The problem with such a long integration time is the lack of charge retention due to leakage through the finite resistance of the photodiode and the OFF-state of the TFT switch. Based on a practical integration time of 20 sec,[19] with a conventional a-Si:H pixel and TFT switch, several successive readouts are required. However, we have developed a new long term charge storage photodetector,[20] which integrates the pixel diode with an external capacitance. This capacitance effectively blocks the leakage current, and makes it possible to integrate charge for 3 min, provided that the thermal generated current in the diode is kept low by operating at low temperature.[20]

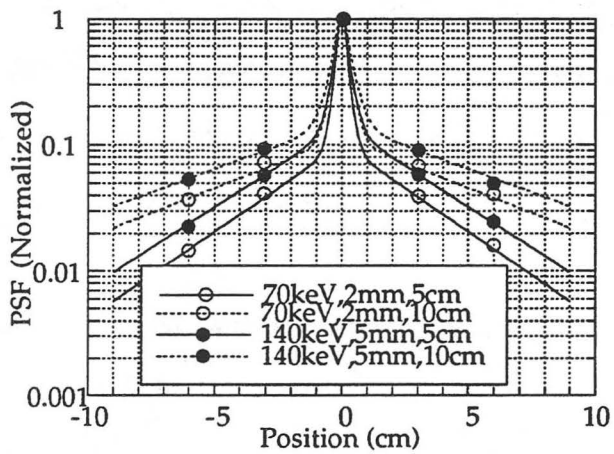

Fig. 7 PSF from a point source in the water phantom with different g energies (70 KeV and 140 KeV), source depths (5 and 10 cm), and scintillator thicknesses (2 and 5 mm).

B. Monte Carlo Simulation

The performance of an a-Si:H based gamma camera was evaluated by a Monte carlo simulation method. For the

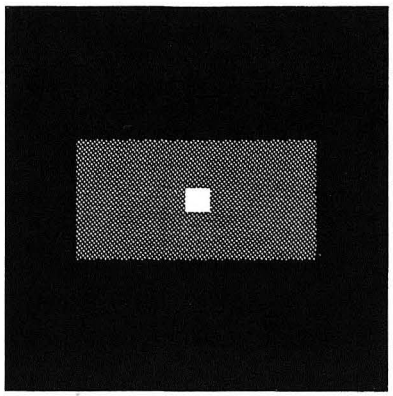

(a)

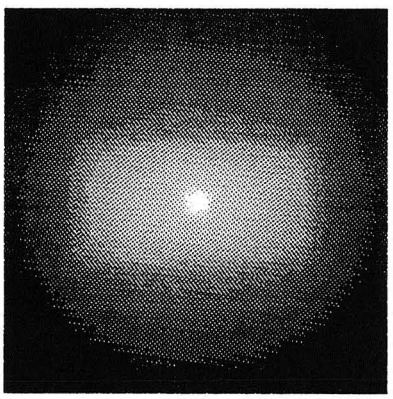

(b)

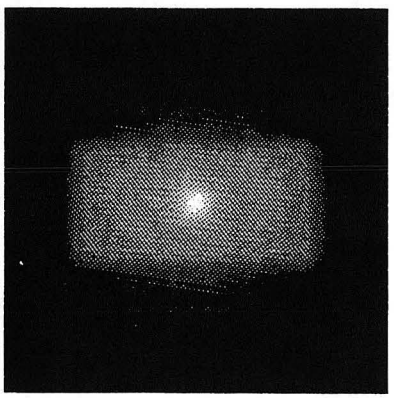

(c)

Fig. 8 Images from simulation: (a) true object, (b) simulated image with a-Si:H based gamma camera, and (c) simulated image with conventional camera.

simulation, ^{99m}Tc (E_γ = 140 KeV) and ^{201}Tl (E_γ = 70 keV) sources were used. Here we briefly describe some of the results, more details on the assumptions and results are given in ref. 21. The analysis shows that for the 70 KeV source, a 2 mm thickness of CsI(Tl) is sufficient to absorb 99% of the γ-rays, and for this thickness of scintillator the spatial resolution of the camera composed of an array of 1x1 mm^2 pixels without any collimation is about 2 mm. However, for the 140 keV source a CsI(Tl) thickness of 5 mm is required and with the same array the resolution is ~ 2.2 mm.

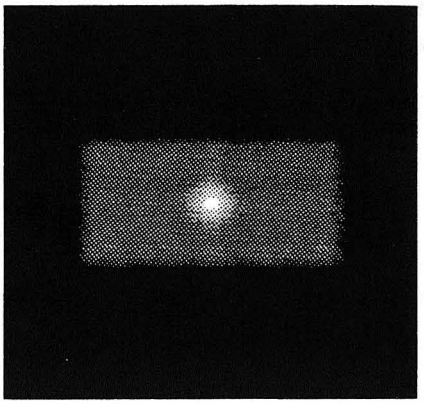

Fig. 9 Restored image using Wiener filter. Image of Fig. 8 (b) with added electronic noise was used as the input image.

A water phantom with three different regions as shown in Fig.6 was used for the simulation. The parameters of the water phantom and the γ-camera are given in Table I. In Fig.7 we show the point spread function (PSF) of the camera for point sources in the water phantom at 5 and 10 cm distances from the collimator surface and γ-ray energies of 70 and 140 keV. For this part of the simulation, warm and hot regions were removed. The peak in the PSF corresponds to response of the camera, whereas the exponential tails are due to the scattering in the phantom. As seen, the slope of the tails depends on the source depth in the phantom and increases with the source-collimator distance. This kind of scattering is also observed in conventional gamma cameras and can be reduced by using an energy window discrimination. In a-Si:H gamma camera (integration mode) such a discrimination is not possible. However, the blurring occurred in the image due to this scattering can be drastically reduced by using an appropriate

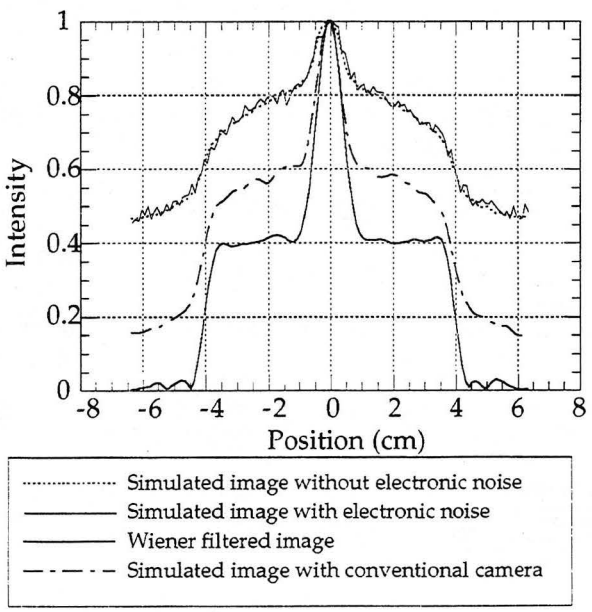

Fig. 10 Profile of images in x-direction. Intensities are normalized to the maximum count.

calculational filter. Figure 8 shows, (a) the true image of the phantom, (b) the simulated Scintigram image with a-Si:H based gamma camera, (c) the simulated image with a conventional camera. The same source (^{99m}Tc) and collimation was used for both cameras and for the conventional camera the parameters of a ZLC75 Siemens camera was used. The blurring effect due to scattering can be restored by applying a Wiener filter.[21] Before restoration, a Gaussian pixel noise of 2 fC was added to the image of Fig. 8b, The result was used as input image in the restoration process. The restored image is shown in Fig. 9. In Fig. 10 we show the profiles of the images in X- direction. As seen from these figure, with restoration, the quality of the image from a-Si:H based gamma camera is even better than that of the conventional camera.

IV. CONCLUSION

Recent advancements in the development of a-Si:H sensor arrays and their integration with associated electronic readouts has made it possible to compete with currently used technology for most applications in the medical imaging. The largest reported array with $3x10^6$ pixels and pixel pitch of 127 μm has good response linearity and high signal to noise ratio. It can be operated under X-ray radiographic or fluoroscopic conditions (30 frames/sec). We have developed a high resolution CsI(Tl) scintillator layer with columnar structures, to enhance light collimation. These layers can be coupled to a-Si:H arrays with high efficiency, by directly evaporating them on the arrays. The structured 110 μm thick CsI(Tl) layers have spatial resolution of ~ 12 lp/mm. We have also evaluated the performance of an a-Si:H based gamma camera, by Monte Carlo simulation. After restoration of the images by Wiener filter, the quality of the simulated image from the camera is better than that of the conventional Anger camera.

ACKNOWLEDGMENT

This work was supported by High Energy Physics Division of U.S. Department of Energy under Contract Number DE-AC03-76SF00098.

REFERENCES

1. W. E. Spear and P. G. LeComber, Philos. Mag. 33 (1976) pp.935-49.
2. S. Kaneko and F. Okumura, "Amorphous Semiconductor Technologies and Devices," ed. Y. Hamakawa, (OHMSA ,1987) pp. 293-302
3. V. Perez-Mendez: *Amorphous and Microcrystalline Semiconductor Devices*, ed. J. Kanicki (Artech House, Boston, 1991) pp. 297-330.
4. A. Mireshghi, G. Cho, J. Drewery, T. Jing, S. N. Kaplan, V. Perez-Mendez and D. Wildermuth, IEEE Trans. Nuc. Sci. NS-39 (1992) pp. 635-40.
5. B. Equer and A. Karar: Nucl. Instrum. & Methods A275 (1989) pp. 558-63.
6. L. E. Antonuk, J. Boudry, Y. El-Mohri, W. Huang, J. Siewerdsen, J. Yorkston, SPIE Physics of Medical Imaging, Vol. 2163 (1994) pp.118-28.
7. L. E. Antonuk, Y. El-Mohri, W. Huang, J. Siewerdsen, J. Yorkston, to be published in Mat. Res. Soc. Symp. Proc. 336 (1994).
8. A..Mireshghi, W. S. Hong, J. Drewery, T. Jing, S. N. Kaplan, H. K. Lee and V. Perez-Mendez, to be published in Mat. Res. Soc. Symp. Proc. 336 (1994).
9. L. E. Antonuk, J. Yorkston, W. Huang, J. Siewerdsen and R.A. Street, Mat. Res. Soc. Symp. Proc. 297 (1993) pp. 945-50.
10. J. Yorkston, L. E. Antonuk, W. Huang and R. A. Street, Mat. Res. Soc. Symp. Proc. 297 (1993) pp. 951-6.
11. N. H. Clinthorne, IEEE Nucl. Sci. Symp. Conf. Rec. Vol. 3 (1993) pp. 1692-6.
12. E. Ellin (Scantech Corp.), Advanced Imaging (1988) pp. 28-32.
13. M. G. Fedotov, E. A. Kuper and V. E. Panchenko, Nucl. Instr.and Meth. Vol. 308, No. 10 (1991) pp. 367-371.
14. G. Cho, J. S. Drewery, W. S. Hong, T. Jing, S. N. Kaplan, H. K. Lee, A. Mireshghi, V. Perez-Mendez, D. Wildermuth, IEEE Trans. Nucl. Sci., NS-40 No. 4 (1993) pp. 323-27.
15. I. Hall, E. Lorenz, G. Mageras, IEEE Trans. Nucl. Sci., NS-35, No. 1 (1988) pp. 105-9.
16. T. Jing, G. Cho, J. Drewery, I. Fujieda, S. N. Kaplan, A. Mireshghi, V. Perez-Mendez and D. Wildermuth, IEEE Trans.Nucl. Sci. NS-39, No.5 (1992) pp. 1195-8.
17. T. Jing, C. A. Goodman, G. Cho, J. drewery, W. S. Hong, H. Lee, S. N. Kaplan, A. Mireshghi, V. Perez-Mendez and D. Wildermuth, IEEE.Nucl. Sci. Symp. Conf. Rec. Vol. 3 (1993 pp. 1878-82.
18. W. R. Hendee: *Medical radiation Physics,* 2nd ed., (Year Book Medical Publishers, 1979) p. 271.
19. I. Fujieda, S. Nelson, R. A. Street and R. L. Weisfield, IEEE Trans. Nucl. Sci., NS-39 (1992) pp. 1056-62.
20. H. Lee, G. Cho, J. S. Drewery, W. S. Hong, T. Jing, S. N. Kaplan, A. Mireshghi, V. Perez-Mendez and D. Wildermuth, Mat. Res. Soc.Symp. Proc., Vol. 297 (1993) pp. 1023-8.
21 H. Lee, J. S. Drewery, W. S. Hong, T. Jing, S. N. Kaplan, A. Mireshghi, V. Perez-Mendez, to be published in SPIE Medical Imaging Conf. Proc. (1994).

LAWRENCE BERKELEY LABORATORY
UNIVERSITY OF CALIFORNIA
TECHNICAL INFORMATION DEPARTMENT
BERKELEY, CALIFORNIA 94720